Effect of surface roughness on metal enhanced fluorescence in planar substrates and optical fibers

Elizaveta Klantsataya,[1,*] Alexandre François,[1,2] Heike Ebendorff-Heidepriem,[1] Beniamino Sciacca,[1,3] Agnieszka Zuber,[1] and Tanya M. Monro[1,2]

[1]*Institute for Photonics and Advanced Sensing, The University of Adelaide, Adelaide, SA, 5005, Australia*
[2]*University of South Australia, Adelaide, SA, 5001, Australia*
[3]*Center for Nanophotonics, FOM Institute AMOLF, Science Park Amsterdam 104, 1098 XG Amsterdam, The Netherlands*
[*]*elizaveta.klantsataya@adelaide.edu.au*

Abstract: We investigate the effect of the roughness of thin silver films on the performance of sensors that exploit metal enhanced fluorescence (MEF). Fluorescence enhancement of dye molecules of up to 47 times was observed on planar glass substrates coated with metal films of higher roughness of around 8 nm. We also study the fluorescence enhancement on the rough silver films implemented on a side of an optical fiber and analyze its dependence on the thickness of the metal. A maximum enhancement factor of 15 was demonstrated for thinner coatings where the film could be considered as a layer of particles. The chemical electroless plating technique used here to produce films with desired roughness is a low cost simple alternative to complex procedures that are currently used for fabrication of nanostructured metal coatings on optical fibers for MEF.

OCIS codes: (290.5880) Scattering, rough surfaces; (160.4236) Nanomaterials; (240.0310) Thin films; (240.6680) Surface plasmons; (260.2510) Fluorescence; (060.2370) Fiber optics sensors.

References and links

1. J. R. Lakowicz, *Principles of Fluorescence Spectroscopy* (Springer, 2006).
2. K. Aslan, I. Gryczynski, J. Malicka, E. Matveeva, J. R. Lakowicz, and C. D. Geddes, "Metal-enhanced fluorescence: an emerging tool in biotechnology," Curr. Opin. Biotechnol. **16**(1), 55–62 (2005).
3. C. D. Geddes, *Metal-Enhanced Fluorescence* (John Wiley & Sons, 2010).
4. J. R. Lakowicz, "Radiative decay engineering 5: metal-enhanced fluorescence and plasmon emission," Anal. Biochem. **337**(2), 171–194 (2005).
5. C. D. Geddes and J. R. Lakowicz, "*Topics in Fluorescence Spectroscopy vol. 8: Radiative Decay Engineering* (Springer, 2007)," Phys. Rep. **113**, 195–287 (1984).
6. A. I. Dragan, E. S. Bishop, J. R. Casas-Finet, R. J. Strouse, J. McGivney, M. A. Schenerman, and C. D. Geddes, "Distance dependence of metal-enhanced fluorescence," Plasmonics **7**(4), 739–744 (2012).
7. J. R. Lakowicz, "Radiative decay engineering: biophysical and biomedical applications," Anal. Biochem. **298**(1), 1–24 (2001).
8. J. R. Lakowicz, Y. Shen, S. D'Auria, J. Malicka, J. Fang, Z. Gryczynski, and I. Gryczynski, "Radiative decay engineering. 2. Effects of Silver Island films on fluorescence intensity, lifetimes, and resonance energy transfer," Anal. Biochem. **301**(2), 261–277 (2002).
9. K. Aslan, S. N. Malyn, Y. Zhang, and C. D. Geddes, "Conversion of just-continuous metallic films to large particulate substrates for metal-enhanced fluorescence," J. Appl. Phys. **103**(8), 84307 (2008).
10. A. L. Feng, M. L. You, L. Tian, S. Singamaneni, M. Liu, Z. Duan, T. J. Lu, F. Xu, and M. Lin, "Distance-dependent plasmon-enhanced fluorescence of upconversion nanoparticles using polyelectrolyte multilayers as tunable spacers," Sci. Rep. **5**, 7779 (2015).
11. K. Aslan, Z. Leonenko, J. R. Lakowicz, and C. D. Geddes, "Annealed silver-island films for applications in metal-enhanced fluorescence: interpretation in terms of radiating plasmons," J. Fluoresc. **15**(5), 643–654 (2005).
12. J. Dostálek and W. Knoll, "Biosensors based on surface plasmon-enhanced fluorescence spectroscopy," Biointerphases **3**(3), FD12–FD22 (2008).

#261697 Received 28 Mar 2016; revised 29 Apr 2016; accepted 2 May 2016; published 27 May 2016

13. Y. Jiang, H. Y. Wang, H. Wang, B. R. Gao, Y. Hao, Y. Jin, Q.-D. Chen, and H.-B. Sun, "Y. wei Hao, Y. Jin, Q.-D. Chen, and H.-B. Sun, "Surface plasmon enhanced fluorescence of dye molecules on metal grating films," J. Phys. Chem. C **115**(25), 12636–12642 (2011).
14. M. Bauch, K. Toma, M. Toma, Q. Zhang, and J. Dostàlek, "Plasmon-enhanced fluorescence biosensors: a review," Plasmonics **9**(4), 781–799 (2014).
15. K. Toma, M. Vala, P. Adam, J. Homola, W. Knoll, and J. Dostálek, "Compact surface plasmon-enhanced fluorescence biochip," Opt. Express **21**(8), 10121–10132 (2013).
16. D. Darvill, A. Centeno, and F. Xie, "Plasmonic fluorescence enhancement by metal nanostructures: shaping the future of bionanotechnology," Phys. Chem. Chem. Phys. **15**(38), 15709–15726 (2013).
17. X. Yu, D. Yong, H. Zhang, H. Li, Y. Zhang, C. C. Chan, H.-P. Ho, H. Liu, and D. Liu, "Plasmonic enhanced fluorescence spectroscopy using side-polished microstructured optical fiber," Sens. Actuators B Chem. **160**(1), 196–201 (2011).
18. K. Arya, Z. B. Su, and J. L. Birman, "Localization of the surface plasmon polariton caused by random roughness and its role in surface-enhanced optical phenomena," Phys. Rev. Lett. **54**(14), 1559–1562 (1985).
19. J. Zhang, E. Matveeva, I. Gryczynski, Z. Leonenko, and J. R. Lakowicz, "Metal-enhanced fluoroimmunoassay on a silver film by vapor deposition," J. Phys. Chem. B **109**(16), 7969–7975 (2005).
20. K. Ray, M. H. Chowdhury, and J. R. Lakowicz, "Use of aluminum films as substrates for enhanced fluorescence in the ultraviolet-blue spectral region," Anal. Chem. **79**, 6480–6487 (2007).
21. H. Raether, *Surface Plasmons on Smooth and Rough Surfaces and on Gratings* (Springer 1988).
22. T. Neumann, M. L. Johansson, D. Kambhampati, and W. Knoll, "Surface-plasmon fluorescence spectroscopy," Adv. Funct. Mater. **12**(9), 575–586 (2002).
23. M. Y. Ng and W. C. Liu, "Fluorescence enhancements of fiber-optic biosensor with metallic nanoparticles," Opt. Express **17**(7), 5867–5878 (2009).
24. A. François, J. Boehm, S. Y. Oh, T. Kok, and T. M. Monro, "Collection mode surface plasmon fibre sensors: a new biosensing platform," Biosens. Bioelectron. **26**(7), 3154–3159 (2011).
25. B. Sciacca, A. François, M. Klingler-Hoffmann, J. Brazzatti, M. Penno, P. Hoffmann, and T. M. Monro, "Radiative-surface plasmon resonance for the detection of apolipoprotein E in medical diagnostics applications," Nanomedicine (Lond.) **9**(4), 550–557 (2013).
26. B. Sciacca, A. François, P. Hoffmann, and T. M. Monro, "Multiplexing of radiative-surface plasmon resonance for the detection of gastric cancer biomarkers in a single optical fiber," Sens. Actuators B Chem. **183**, 454–458 (2013).
27. J. Boehm, A. François, H. Ebendorff-Heidepriem, and T. Monro, "Chemical deposition of silver for the fabrication of surface plasmon microstructured optical fibre sensors," Plasmonics **6**(1), 133–136 (2011).
28. R. S. Sennett and G. D. Scott, "The structure of evaporated metal films and their optical properties," J. Opt. Soc. Am. **40**(4), 203–211 (1950).
29. E. Palik, *Handbook of Optical Constants of Solids* (Elsevier 1998).
30. G. Decher, "Fuzzy nanoassemblies: toward layered polymeric multicomposites," Science **277**(5330), 1232–1237 (1997).
31. F. Caruso, K. Niikura, D. N. Furlong, and Y. Okahata, "Ultrathin multilayer polyelectrolyte films on gold: construction and thickness determination," Langmuir **13**(13), 3422–3426 (1997).
32. B. D. Gupta and R. K. Verma, "Surface plasmon resonance-based fiber optic sensors: Principle, probe designs, and some applications," J. Sens. **2009**, 1–12 (2009).
33. A. K. Sharma and B. Gupta, "Theoretical model of a fiber optic remote sensor based on surface plasmon resonance for temperature detection," Opt. Fib. Tech. **12**(1), 87–100 (2006).
34. J. E. Wong, F. Rehfeldt, P. Hanni, M. Tanaka, and R. Klitzing, "Swelling behavior of polyelectrolyte multilayers in saturated water vapor," Macromolecules **37**(19), 7285–7289 (2004).
35. A. D. Rakić, A. B. Djurišić, J. M. Elazar, and M. L. Majewski, "Optical properties of metallic films for vertical-cavity optoelectronic devices," Appl. Opt. **37**(22), 5271–5283 (1998).
36. P. Pavaskar, J. Theiss, and S. B. Cronin, "Plasmonic hot spots: nanogap enhancement vs. focusing effects from surrounding nanoparticles," Opt. Express **20**(13), 14656–14662 (2012).
37. H. Cang, A. Labno, C. Lu, X. Yin, M. Liu, C. Gladden, Y. Liu, and X. Zhang, "Probing the electromagnetic field of a 15-nanometre hotspot by single molecule imaging," Nature **469**(7330), 385–388 (2011).
38. B. J. Messinger, K. U. von Raben, R. K. Chang, and P. W. Barber, "Local fields at the surface of noble-metal microspheres," Phys. Rev. B **24**(2), 649–657 (1981).

1. Introduction

Fluorescence analysis has been a dominant technique in biochemical sensing and medical diagnostics studies due its high sensitivity, simplicity, and availability of fluorophores. However, there is a drive to further improve detection limits as fluorophores detectability is eventually limited by their quantum yield, photostability and autofluorescence [1]. In the last decade Metal Enhanced Fluorescence (MEF) has attracted significant attention as an emerging tool for fluorescence spectroscopy, alleviating the aforementioned issues by

#261697 Received 28 Mar 2016; revised 29 Apr 2016; accepted 2 May 2016; published 27 May 2016

enhancing fluorescence emission and decreasing fluorescence lifetime thereby improving fluorophore detectability [2].

Noble metal particles and planar surfaces exhibit diverse and complex optical properties associated with Surface Plasmons (SPs), which can be described as light-induced collective electron oscillations on metallic thin film surfaces or nanoparticles. The electromagnetic field associated with SPs is at maximum at the interface and decays exponentially in the direction perpendicular to that interface. MEF is attributed to the stronger interactions occurring between fluorophores' excited states and the induced SPs in metal particles or films due to the increased electromagnetic field in the proximity of the metals [3–5]. Therefore, the effect of metal surfaces and particles on fluorophores depends on both the distance separating the fluorophore molecules from the metal and the overlap between the SPs resonance wavelength and the fluorophore absorption [6,7]. Earlier studies have shown that metals can be used to modify the fluorescence intensity (quenching or enhancement), decrease or increase the radiative decay rates, and improve the photostability [2–9].

Nanostructured metal films and nanoparticles have been extensively studied for MEF [10–16]. The enhancement factors depend on the type, shape, size, and separation between nanoparticles, and enhancement values from 10 to 10^6 have been reported for some configurations. However, it remains experimentally challenging to produce large-scale nanostructured surfaces with consistent surface coverage density to achieve reproducible MEF properties [17]. Continuous smooth metal films, while simpler to produce, exhibit dramatically lower enhancement factors, typically on the order of 2 [18]. For this reason, there has been significant interest in studying rough metal surfaces with the intention to bridge the performance gap between metal nanostructures and continuous films, as described below.

The SPs on a rough surface undergo elastic scattering due to the spatial fluctuation in the dielectric function of the metal-dielectric interface. This results in localization of SPs and increased electromagnetic field amplitude near the rough surface in comparison to the field supported by a smooth film [19]. MEF suitable films reported previously have been achieved by annealing of thermally evaporated silver films to produce cracks [12], by using a slow thermal evaporation rate during silver deposition [20], or fabricating very thin particulate metal films [21]. The majority of the MEF experiments are performed on planar substrates with the fluorophore being excited through the SPs. Measurement of such substrates are traditionally performed using attenuated total reflection (ATR) in a prism, also known as Kretschmann configuration, to match the propagation constant of the excitation light with that of the SPs at a given angle of incidence [13,23]. Although this approach offers high resolution and simple experimental realization, it is somewhat cumbersome, expensive, and is not applicable for remote sensing. To overcome those issues, waveguides and fiber based MEF configurations that offer advantages of easy coupling, miniaturization, and potential for multiplexing have been proposed [18,24].

In this paper, we investigate the influence of surface roughness of continuous silver films on fluorescence enhancement in planar glass substrates. Silver films of thicknesses around 50 nm with varying roughness from 2 nm to 8 nm were prepared by two methods, thermal vapor deposition and chemical electroless plating. As the plasmonic enhancement of fluorescence depends on the separation between the fluorophore and the metal [2–4,7,11], the optimal distance that provides maximum enhancement at a given roughness was achieved through layer-by-layer deposition of a polyelectrolyte multilayer spacer. Fluorescence intensity was found to increase for coatings with higher surface roughness. Based on the determined optimal surface roughness and the spacing between the fluorophore and the metal film, we demonstrate the fabrication of MEF based sensor on a side of a multimode optical fiber. It was previously reported that a fiber configuration with a rough silver coating could be used for fabrication of radiative Surface Plasmon Resonance (SPR) sensors that exploit scattering of the plasmonic wave [25–27]. Building on this SPR fiber sensing platform, we study the

#261697 Received 28 Mar 2016; revised 29 Apr 2016; accepted 2 May 2016; published 27 May 2016

dependence of fluorescence intensity on the thickness of the silver films and discuss advantages and limitations of the MEF fiber sensor.

2. Experimental section

2.1. Silver film fabrication

To investigate the dependence of fluorescence intensity on the roughness of the silver coating and determine the optimal distance between the fluorophore and the metal film, we first performed experimental studies in planar geometry. Silver thin films of 50 nm thicknesses, previously determined to be optimal for SPs excitation [28], were deposited on standard microscope glass slides using two methods, electroless plating [28], and thermal evaporation [29]. Different deposition conditions, in particular deposition rates, were used for the thermal evaporation to vary the surface roughness of the deposited silver films [29]. Procedure reported by Boehm *et al.* [28], was followed for fabrication of silver coatings using the electroless plating method. All substrates were thoroughly cleaned by sonication in acetone for 30 min, then rinsed with ethanol and deionized water prior silver thin film deposition. Thermal vacuum evaporation was performed in thermal evaporator (JEOL JEE 420) with a tungsten crucible at a pressure of 2×10^{-4} Pa. The current was varied from 28 to 40 Amps, resulting in deposition rate ranging from 0.32 to 3.52 nm/s to produce coating with a range of surface roughness.

Silver electroless plating was also used to fabricate silver films on a side of a multimode lead silicate optical fiber (F2, refractive index of 1.62 at 633 nm) with a core diameter of 160 μm. To produce MEF fiber sensors, a 1-cm long section of the fiber was stripped off the polymer cladding to allow for silver film deposition onto the fiber core. Fiber samples with different silver film thicknesses of 71, 56, 35 and 22 nm have been produced to analyze the effect of coating thickness on fluorescence enhancement.

2.2. Silver film characterization

The thickness of the deposited silver films on the planar substrates was measured using transmission measurements with a helium neon (HeNe) laser (λ = 633 nm). Calculation of the coating thickness (t) has been carried out using the Beer-Lambert law: $I = I_0 e^{-t\alpha}$, where I_0 and I are the incident and transmitted power respectively, and α = 756310 cm^{-1} is the absorption coefficient of silver at 633 nm [30]. Due to the surface roughness of the metal films, which introduces scattering losses, as well as the reflection from the surfaces, the amount of light detected in transmission is reduced, which might result in overestimates of the film thickness. To evaluate the scale of these effects, the metal film thickness for some samples was also measured using atomic force microscopy (AFM) (NT-MDT) at the edge of the coatings. AFM estimated thicknesses were found to lie within the uncertainty ranges of the values calculated using transmission measurements, which indicates that the transmission method could be used as a simple and fast alternative for measuring the metal film thickness. Topography of the fabricated metal coatings and film roughness were also studied using AFM. Surface roughness values presented in the manuscript are root mean square roughness defined as the average of height deviations measured from the mean line and taken within the evaluation length, and was estimated using scanning probe microscopy data analysis software (Nova NT-MDT and Gwyddion). The results for the metal film thickness, surface roughness and deposition rate for coatings prepared using the two methods are summarized in Table 1.

#261697 Received 28 Mar 2016; revised 29 Apr 2016; accepted 2 May 2016; published 27 May 2016

Table 1. Properties of the different silver films

Deposition method	Thickness (nm)	Deposition rate (nm/s)	Roughness (nm)
Experiment with planar substrates (Kretschmann setup)			
Thermal evaporation, 28 Amps	46.5 ± 1.5	0.32	4.1 ± 0.4
Thermal evaporation, 30 Amps	51.4 ± 3.4	0.73	2.8 ± 0.7
Thermal evaporation, 36 Amps	50.7 ± 0.5	2.29	2.5 ± 0.1
Thermal evaporation, 40 Amps	49.8 ± 0.1	3.52	1.7 ± 0.2
Chemical electroless plating	53.0 ± 5.0	0.12	7.9 ± 0.6
Samples used for fibre coating characterization			
Chemical electroless plating	22.4 ± 2.2	0.08	8.8 ± 0.6
Chemical electroless plating	34.9 ± 2.9	0.15	9.1 ± 0.4
Chemical electroless plating	56.3 ± 3.4	0.13	11.0 ± 0.7
Chemical electroless plating	71.1 ± 2.5	0.15	9.4 ± 0.1

2.3. Surface functionalization

The distance between the silver film and the fluorophore was finely tuned through layer-by-layer adsorption of positively and negatively charged polyelectrolyte (PE) layers, poly(allylamine hydrochloride) (PAH) and (poly(sodium 4-styrenesulfonate) (PSS) respectively [31]. PE solutions of 2 mg/mL were prepared in 1M of aqueous sodium chloride. The samples were immersed in each PE solution for 15 min and rinsed in deionized water between each step. Planar glass substrates with odd number of PE layers ranging from 1 to 21 and starting from PAH layer were prepared to vary the gap between the metal film and the fluorophore with each PE layer adding 1.7 ± 0.1 nm separation, as described in Section 3.1. Fiber samples were prepared using the same protocol. It has previously been reported that PE layer formation follows uniform growth after deposition of four layers, and even a small amount of PAH is sufficient to facilitate subsequent adsorption of PSS [32]. Therefore, it can be assumed that thickness and density of polyelectrolyte for multiple layers is independent on the substrate. A carboxyl functionalized organic fluorescent dye (4-(2-Carboxyphenyl)-7-diethylamino-2-(7-diethylamino-2-oxochroman-3-yl)-chromylium perchlorate) (λ_{ex}~650 nm, λ_{em}~690 nm) was covalently attached to the last PAH layer using amine coupling reagents, 1-Ethyl-3-(3-dimethylaminopropyl)carbodiimide (EDC) and N-Hydroxysuccinimide (NHS). A concentration of 10.9 mg of the organic dye in 10 mL of water and 5 mL of methanol was used.

2.4. Experimental setup

A Kretschmann prism was set up as depicted in Fig. 1(a) with a BK7 prism mounted on a computer controlled rotational stage and a linearly polarized 633 nm HeNe laser as an excitation source. This configuration was used for characterizing surface plasmon fluorescence enhancement on the planar substrates. The minimum in the reflected spectrum as a function of the incidence angle of the excitation light that corresponds to the surface plasmon resonance was monitored with a power meter on the opposite side of the prism. The fluorescent signal was collected from the fluorophore coated glass slide surface with a × 10 microscope objective. After removing the excitation light with a 650 nm long pass filter, the fluorescent signal was analysed with a compact spectrometer (Ocean Optics QE 65000).

Silver coated optical fiber sensors were enclosed in a glass tube to allow liquid to flow around the sensing region as shown in the Fig. 1(b). A short section of the fiber polymer cladding near the silver coating was removed to create an uncoated region for comparison. Having both silver coated and uncoated parts of the sensor inside one flow cell ensured both regions undergo the same surface functionalization procedure. The sensitivity of surface

#261697 Received 28 Mar 2016; revised 29 Apr 2016; accepted 2 May 2016; published 27 May 2016

plasmon resonance (SPR) response has been characterized by flowing aqueous solutions of glycerol with known refractive indices through the flow cell. A white light LED (Thorlabs Inc., MCWHL2) was used for SPR analysis. A presence of significant surface roughness of the metal coating allowed for analysis of light scattered by surface plasmons directly above the sensor surface [25–27] instead of transmission measurements as it is done in conventional SPR fibre sensors [33]. PE layer deposition and dye attachment on the fiber samples were performed inside the flow cell and the SPR response was recorded at each step of the functionalization process. The fluorescence measurement setup shown in Fig. 1(b) is similar to the described SPR configuration with a monochromatic HeNe laser source used for fluorophore and plasmon excitation. The fluorescent signal was collected above the sensing region with a collection apparatus consisting of microscope objective, converging lens, and an optical fibre, and analysed with the Ocean Optics compact spectrometer. A long pass filter (650 nm) was used to block laser background radiation.

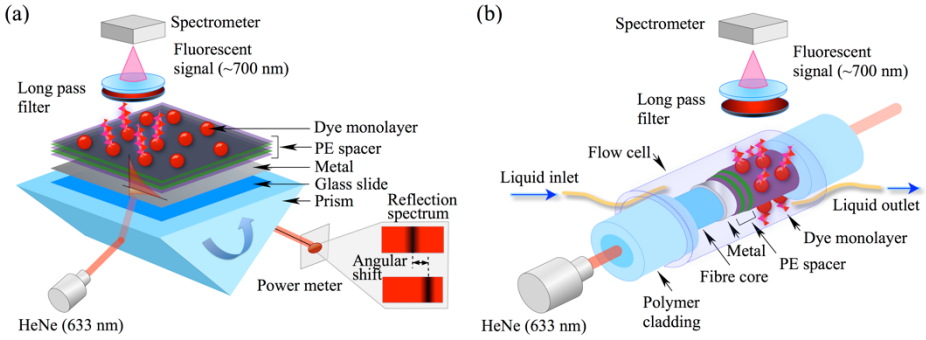

Fig. 1. Schematic of the optical setup for surface plasmon fluorescence enhancement analysis on (a) planar substrates; and (b) optical fibers.

3. Results and discussion

3.1 Surface roughness dependent fluorescence enhancement in planar substrates

A typical SPR response on planar substrates is presented in Fig. 2(a). Upon adsorption of the PE multilayers, the minimum in the reflected light that corresponds to the plasmon resonance is shifted towards higher incidence angles. Figure 2(b) shows the SPR signal and the corresponding fluorescence signal with the maximum fluorescence intensity occurring at the resonance, which is seen as a dip in the reflected light.

The fluorescence enhancement factor (*EF*) is defined as the ratio of maxima of fluorescence intensities of silver (Ag) coated substrate and an uncoated substrate: $EF = I_{coated}/I_{uncoated}$. For all samples coated with silver using thermal evaporation method the maximum fluorescence enhancement occurred after deposition of 7 PE layers. This corresponds to a distance of approximately 12.0 ± 0.8 nm, as shown in the Fig. 3(a) which illustrates the dependence of fluorescence enhancement factor in planar substrates with silver films of different surface roughness as a function of the number of deposited PE layers. The thickness of the PE coating was determined from the SPR response using multilayer model described elsewhere [34], and assuming the refractive indices of glass and PE coating being 1.54 and 1.47 respectively [35], and a complex dielectric function of silver estimated using Lorentz-Drude model [36]. Even though the dielectric function of thin films could differ from that of bulk metal, the Lorentz-Drude model can be used to obtain a rough estimate of the PE layers thickness, which is broadly consistent with previously reported thickness of individual PE layers of ≈1.5 nm [31,32,35]. For the slides with silver coating deposited by chemical method the SPR angular shift was larger than for samples with thermally evaporated coatings.

#261697 Received 28 Mar 2016; revised 29 Apr 2016; accepted 2 May 2016; published 27 May 2016

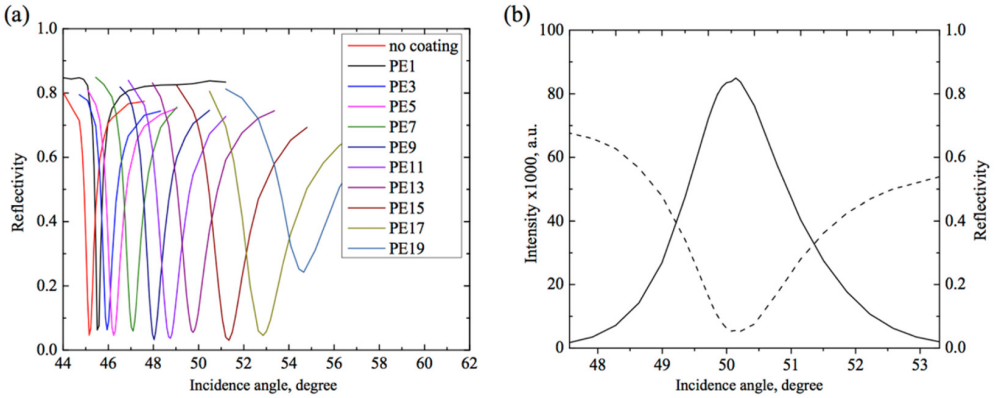

Fig. 2. (a) A typical increase in the angular position of the dip in the reflected spectra corresponding to Surface Plasmon Resonance (SPR) as a function of increasing number of polyelectrolyte layers on a planar substrate; and (b) Fluorescence emission of the dye (solid line) and SPR signal (reflectivity) (dashed line) of a planar substrate. A sample with thermally evaporated coating was used as an example.

This could be attributed to the difference in the dielectric function of silver deposited by chemical technique versus thermally evaporated silver, or could be related to the stronger interaction of the SPs with the environment due to the surface roughness. Nevertheless, the maximum fluorescence enhancement factor for chemically coated glass slides was observed after deposition of 7 PE layers. Figure 3(b) shows the maximum fluorescence enhancement factor as a function of silver coatings' roughness. It demonstrates that fluorescence enhancement increases as the surface roughness of the Ag film increases, ranging from the factor of 3 for low surface roughness of 1.7 nm up to the factor of 47 for the roughness of 8 nm.

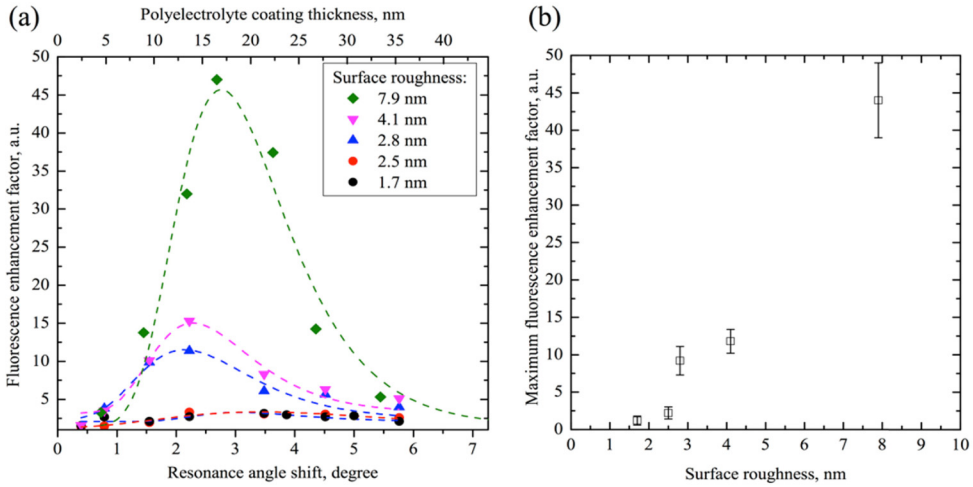

Fig. 3. (a) Dependence of fluorescence enhancement factor of planar substrates coated with silver coating of different surface roughness as a function of PE spacer thickness; and (b) Maximum fluorescence enhancement factor as a function of silver coatings roughness.

The fluorescence enhancement on a rough surface is thought to occur due to the presence of hot spots in the near field due to the larger local density of optical states. When the random surface texture consists of a collection of metal nanoparticles located in a nanoscale distance from each other, SPP field overlaps creating strongly confined electromagnetic modes. This phenomenon is associated with surface enhancement effects such as surface enhanced Raman

#261697 Received 28 Mar 2016; revised 29 Apr 2016; accepted 2 May 2016; published 27 May 2016

scattering and is believed to be responsible for the enhancement of fluorophore excitation [37,38].

3.2 Fluorescence enhancement in an optical fiber

Fluorescence enhancement was also investigated on an optical fiber coated with silver film fabricated using the electroless plating as the rough coating produced with this method showed higher enhancement factor. Typical SPR scattered spectra are depicted in Fig. 4 showing a spectral shift occurring after each step of surface functionalization process. The initial observed fluorescence enhancement factor for the fiber-based configuration was found to be 2.4, which is significantly lower than the factor of 47 achieved on the planar substrates.

This difference can be explained by considering that there is a spectral mismatch between SPR excitation wavelength after the completion of surface functionalization process (around 580 nm, black vertical line in Fig. 4) and the excitation wavelength of the fluorophore (633 nm, red vertical line in Fig. 4). While Kretschmann based systems can easily compensate for this discrepancy by changing the incidence angle ensuring that the propagation constants of both the incident light and the plasmons are always matched, this is not possible for an optical fiber based approach where the range of incidence angles are limited by numerical aperture of the fibre. This suggests that in a fiber based MEF configuration a careful selection of a fluorescent dye is more critical due to the necessity of maximizing the overlap between excitation spectrum of the dye and SPR associated signal. While in practice this introduces a restriction, the thickness of the silver film can be altered to further increase the fluorescence enhancement as shown by Zhang *et al.* [20].

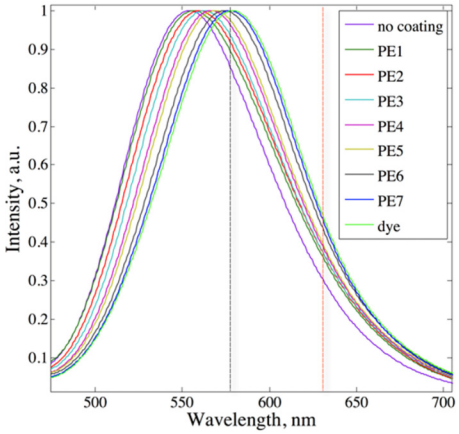

Fig. 4. Normalized scattered SPR signal at each step of the surface functionalization process (PE spacer deposition and dye attachment) on a side of an optical fiber coated with 56 nm silver film. Vertical lines mark the SPR resonant wavelength after dye attachment at around 580 nm (black) and the excitation wavelength of the laser source at 633 nm (red).

To explore this further, we investigated the dependence of fluorescence enhancement on the thickness of the silver coatings fabricated on a side of an optical fiber by chemical deposition, and performed analysis of the topography of the deposited films. We examined the fluorescence enhancement factor for silver films of 71, 56, 35, and 22 nm thicknesses. All films were fabricated using the same chemical electroless plating procedure with varying reaction time keeping the deposition rate constant. This allowed for fabrication of films of different thicknesses without significantly changing the surface structure, in particular, surface roughness. The thickness of the coatings on the fibre samples was estimated by AFM on planar glass substrates that were prepared together with the fibre samples at the same deposition rate. It has been found that fluorescence is quenched on fibres coated with thick films (71 nm) and is enhanced on thinner films (≤ 56 nm) as shown in the Fig. 5(a).

#261697 Received 28 Mar 2016; revised 29 Apr 2016; accepted 2 May 2016; published 27 May 2016

Significantly larger enhancement factors were obtained on thin films reaching up to 15-fold for the thinnest film studied (Fig. 5(b)), while the standard 56 nm-thick silver film exhibited only a 2-fold increase of the fluorescence intensity.

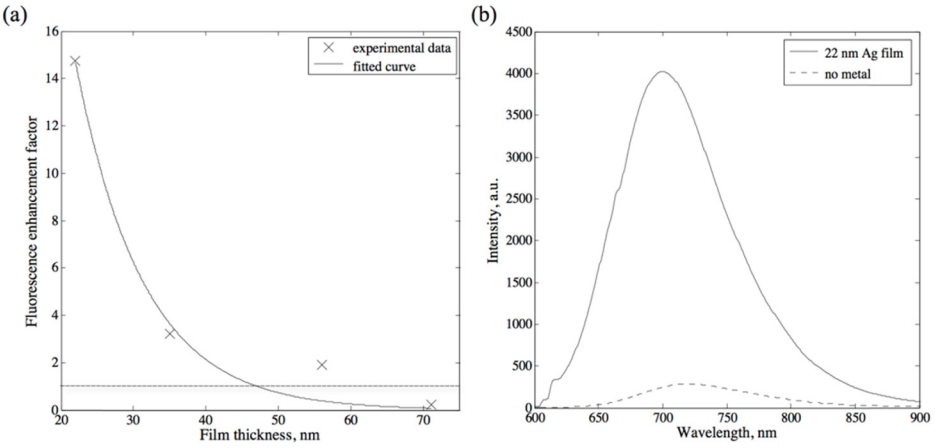

Fig. 5. (a) Fluorescence enhancement factor for varying silver film thickness in fiber samples. Fluorescence enhancement factor above one indicates fluorescence intensity enhancement, below one - reduction of fluorescence intensity; and (b) Fluorescent signal for a fiber coated with 22 nm silver film (solid line), and without metal (dashed line).

The extinction properties of metals depend on both absorption and scattering components [4]. According to Mie theory, the ratio of scattering to total extinction of small metal particles is small, which means that a large fraction of incident light is absorbed, leading to inefficient excitation of fluorophores nearby. On the other hand, in larger metal nanostructures the fraction of light scattered by the particles is increased, which is expected to favor fluorescence enhancement [38]. Surface scattering depends not only on amplitude roughness parameters, such as the root mean square roughness, but also on spatial roughness parameters given by autocorrelation function. The analysis of AFM images was performed to understand the difference in terms of surface features between the 22 and 71 nm silver films. Figures 6(a) and 6(b) show the distribution of equivalent disk radius r_{eq} (radius of a disk with the same projected area as the grain) of thin (22 nm) and thick (71 nm) Ag films on 5 × 5 μm sections with AFM images and statistics of the grain composition presented on the insets. Root mean roughness and autocorrelation lengths for both films were found to be the same within their uncertainty estimates. The analysis suggests that the mean size of the surface features does not change significantly with increasing thickness of the metal films with estimated values of 53.6 ± 2.7 nm to 59.6 ± 4.4 nm for 22 and 71 nm films respectively, confirming that the surface roughness remains unchanged with the range of the thicknesses studied, as long as the deposition rate is kept constant. Composition of particles of different size on the surface is similar for thin and thick coatings with around 35% of the particle populations consisting of small features, around 10 nm radius (large peaks on Figs. 6(a) and 6(b)). However, for the 22 nm film, the relative roughness is around half of the film thickness with the gaps between particles reaching down to a few nanometers depth. This film could be considered as a layer of nanoparticles of various sizes. On the other hand, the thick silver film (71 nm) with the relative surface roughness of around tenth of the film thickness could be visualized as a continuous film. For the thick films the intrinsic absorption in metal is stronger than that in the thinner films which results in less efficient excitation of the fluorophores, and thereby, smaller fluorescence emission intensity.

#261697 Received 28 Mar 2016; revised 29 Apr 2016; accepted 2 May 2016; published 27 May 2016

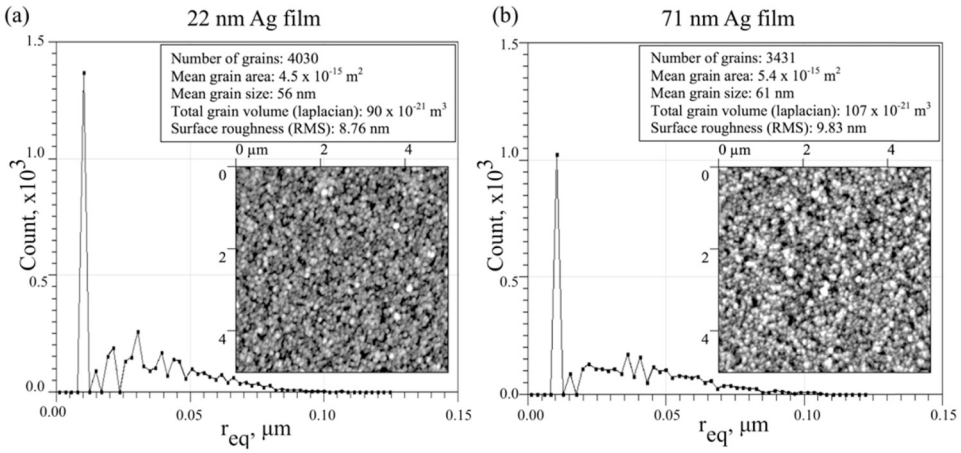

Fig. 6. Particle distribution analysis of thin and thick silver films for 5 × 5 µm sections. Equivalent disk radius (r_{eq}) of the surface features on (a) 22 nm and (b) 71 nm silver films. Statistics of the grain analysis of the coatings as well as AFM images of surface topography are shown on the insets.

In addition to the analysis of the silver film thickness and surface topography, and their influence on enhancement of the fluorescence emission, we performed a simple study of how the fluorescence enhancement depends on the position of the sensing region from where the fluorescent light is collected. Figure 7(a) shows an example of fluorescent signal taken from three different locations on a fiber sensor, a few mm lengths each. As shown schematically in Fig. 7(b), the first fluorescence spectra is collected from a location on the fiber without metal coating, the second from a location at the beginning of the metal coated region, and the third was taken from a location on the metal coated region further away from the fiber end where the light is coupled.

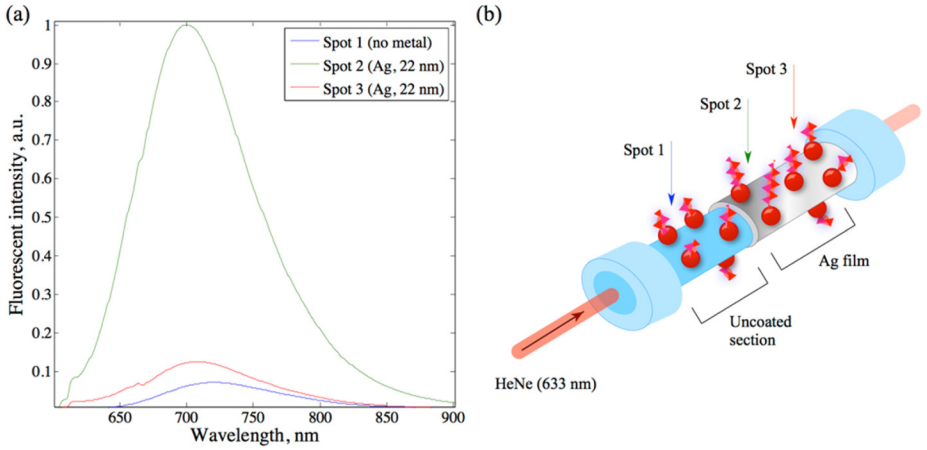

Fig. 7. (a) Comparison of fluorescence intensities from different locations on a fiber coated with 22 nm Ag film and an uncoated section; and (b) Locations of the spots on the fiber sensor.

The results indicate that the fluorescence enhancement strongly depends on the position on the metal-coated region, with higher fluorescence intensities observed at the start of the sensing region where more of the excitation light interacts with the metal. The incident light dissipates quickly through coupling to plasmonic modes and strong scattering enhanced by the roughness of the metal surface. This illustrates that in a fiber-based configuration where

#261697 Received 28 Mar 2016; revised 29 Apr 2016; accepted 2 May 2016; published 27 May 2016

the interaction of propagating light and SPs occurs along the length of the sensing region, intensity of the fluorescent signal is strongly position dependent, and therefore, the detection ideally needs to be integrated over a reasonably large area.

4. Conclusion

In this study, we have investigated the influence of the surface roughness of silver films on the enhancement of emission of fluorophore molecules located at a nanoscale distance from the metal surface. An optimal separation between the fluorophore and the silver film for the maximum enhancement was adjusted by tuning the thickness of a multilayer polyelectrolyte spacer. The maximum fluorescence enhancement factor of up to 47 was achieved on planar glass substrates coated with silver film with significant surface roughness of around 8 nm that was fabricated by a simple electroless plating technique. While this enhancement factor is relatively moderate in comparison to those achieved with nanostructured metal films, it demonstrates that the simple chemical method could be readily used for fabrication of low cost alternative plasmonic coatings suitable for enhancing fluorescence intensity by significant amount when compared with smooth metal films.

We have applied the same silver coating and surface functionalization processes to produce MEF sensors on a side of an optical fiber in order to investigate the prospect of establishing a MEF fibre sensing platform using a straightforward manufacturing technique. The constraints imposed by the fiber geometry significantly reduce the enhancement factor. Indeed, since this configuration removes the ability to tune the incidence angles of the propagating rays onto the metallic coating in optical fibers, the fluorophore has to be carefully chosen to achieve maximum overlap between SPR and fluorophore absorption spectra. Considering this, using fluorescent labels with broad absorption spectrum, such as quantum dots, might be a more suitable option in fibre based MEF sensors. The thickness of the deposited thin film can be reduced to alleviate some of these limitations enabling up to 13-fold increase of the fluorescence emission for a 22 nm thick silver film when compared to an enhancement factor of 2 for a 56 nm film. Finally, we have shown that the length of the metallic coating in optical fibres and the position from where the fluorescence signal is collected, strongly influence the results. It is worth mentioning that this enhancement factor of 15-fold was obtained using a relatively simple fabrication technique and is 7-fold higher than that previously achieved in optical fibre MEF sensors [18]. The MEF fiber sensor could find potential applications in biotechnology, clinical assays and analytical chemistry. The fabrication and analysis procedures are easily adaptable and inexpensive making the fiber MEF sensor a competitive candidate for compact fluorescence spectroscopy.

Acknowledgments

The authors acknowledge the support of Tanya M. Monro's ARC Georgina Sweet Laureate Fellowship and the support of the ARC Centre of Excellence for Nanoscale BioPhotonics. This work was performed in part at the OptoFab node of the Australian National Fabrication Facility utilizing Commonwealth and SA State Government funding.

#261697 Received 28 Mar 2016; revised 29 Apr 2016; accepted 2 May 2016; published 27 May 2016